

# **Mg Magnesium Technology 2012**

**Advanced Processing and Joining**  
**Thursday AM**

***Session Chairs:***

**Tyrone Jones**  
**(U.S. Army Research Laboratory, USA)**

**Brian Jordan**  
**(University of Alabama, USA)**

## MICROSTRUCTURE AND CREEP PROPERTIES OF MEZ MAGNESIUM ALLOY PROCESSED BY THIXOCASTING

Emma D. Morales Garza, Hajo Dieringa, Norbert Hort, Karl. U. Kainer

Helmholtz-Zentrum Geesthacht Centre for Materials and Coastal Research, Max-Planck-Straße 1, 21502 Geesthacht, Germany

Keywords: MEZ magnesium alloy, semi-solid processing, thixocasting, creep, microstructure

### Abstract

Whereas in most magnesium applications die casting is the dominant manufacturing process, thixocasting recently came into focus of producers. This is mainly due to the improved microstructure, reduced porosity and better mechanical properties. An important issue for the introduction and use of magnesium alloys in automotive industry is their creep resistance. Aluminum free magnesium alloys are known to show improved creep strength compared to conventional aluminum containing alloys due to the absence of beta phase ( $Mg_{17}Al_{12}$ ). MEZ alloy (Mg-RE-Zn-Zr) shows better creep resistance even compared to AE42 in die casting. In this paper, the mechanical and creep properties from thixocast MEZ alloy are evaluated from creep tensile tests at temperatures of 135°C, 150°C and 175°C and at stresses between 60 and 100 MPa. The creep activation energy and the stress exponent are calculated and discussed. Optical, scanning and transmission electron microscopy of the microstructural features developed after the mechanical tests helps to understand the deformation mechanisms occurring during creep and to explain the creep properties after thixocasting.

### Introduction

Environmental awareness demanding the reduction of fuel consumption has been the driving force for the renaissance of magnesium alloys in the automotive industry in the last decades. The currently used magnesium components are made with conventional alloys (AM and AZ alloys) and are mainly manufactured by high pressure die casting processes. These alloys, however, are prone to creep above temperatures of 120°C, precluding their use from further automotive applications, e.g. power train components, such as engine blocks and automatic transmission cases, where the operative temperature can approach or even exceed 150°C [1, 2]. The search after better high temperature creep resistant magnesium alloys continues and therefore, different alloying systems have been proposed through the years, most of them excluding aluminum but including rare earth elements or heavy rare earth elements, systems that might reach excellent creep properties, but that are expensive and/or difficult to cast. Low-cost alternative candidates are Zn-based magnesium alloys enhanced with rare earths and/or calcium, but alloys based on these systems have shown limited castability due to the high shrinkage of the Mg-Zn system during conventional casting [3]. As a result, other casting processes, like semi-solid processing, are under research for these magnesium alloys. Thixocasting constitutes an alternative process because of lower energy consumption, net-shapes formed parts, lower porosity and fine microstructures. Nevertheless, the need of special precursor materials with thixotropic properties has kept away the interest of the automotive sector because of the high implied costs in their production. Therefore, thixocasting of magnesium alloys for automotive applications remains as an unexplored field.

### Experimental

The composition of the feedstock material used for the thixocast experiments is presented in Table I. The MEZ alloy was prepared and supplied by Magnesium Elektron Ltd. The material was received as extruded bars, which were heated up to the semi-solid state by means of induction without stirring and subsequently poured manually into the shot sleeve of a vertical Squeeze-Casting machine (UBE HVSC 350, property of LKR Leichtmetallkompetenzzentrum). Previous works on magnesium alloys have shown the feasibility of using extruded material for the production of spheroidized microstructure after semi-solid processing [4, 5]. The reheating temperature of the extruded bars was chosen as 640°C to assure the formation of semi-solid slurry before pouring (with 40 to 60% solid fraction). The final products were stepped plates with dimensions of 110 mm x 250 mm and thicknesses of 2, 6, 10 and 14mm.

Table I. Composition of the MEZ extruded bars (in wt. %) as reported by the supplier (MEL), magnesium based.

Al	Fe	Mn	Ni	Zn	Zr	RE	Others
<0.01	0.003	0.13	0.001	0.4	0.12	2.6	<0.01

Round creep specimens were machined from the 10 and 14 mm steps of the MEZ alloy in the thixocast state. Creep tensile tests were conducted at constant stresses of 60, 70, 80, 90 and 100 MPa and temperatures of 135, 150, and 175°C. In order to characterize the microstructural features of the alloy, the crept samples were embedded in epoxy resin. The specimens were then ground with SiC grit paper and polished with OPST<sup>TM</sup>. After the metallographic preparation, the samples were etched chemically for the purpose of contrasting grain boundaries by means of optical microscopy. The etching solution was prepared after Kree [6]. The microstructure of the samples after chemical etching was studied using a Leica upright optical microscope type DM LM equipped with polarization filters and a Nikon digital camera type DM1200. A Zeiss Scanning Electron Microscope model DSM 962 was used to reveal the microstructure of the alloys at higher magnifications and to obtain chemical information of the phases developed in the material. Transmission electron microscopy observations were performed on a JEOL 2000 coupled with an energy dispersive X-ray analysis (EDX) system operating at 200 kV.

### Results

#### Microstructure of the Extruded Feedstock Material

The microstructure of the as-received extruded MEZ material is presented in Figure 1. The average grain size is quite heterogeneous in the transversal section of the extruded bars ( $10 \mu\text{m} \pm 7 \mu\text{m}$ ), while the extrusion direction is characterized by a strong bimodal grain size distribution with elongated and

equiaxed grains. The X-ray diffraction pattern shows only two dominant phases in the extruded condition: the  $\alpha$ -Mg and the  $Mg_{12}RE$ , Figure 2. SEM-EDX analysis confirms the presence of both phases and also the presence of particles of  $Mn_2Zr$ , which appear sparingly and combined with the  $Mg_{12}RE$  phase, Figure 3.

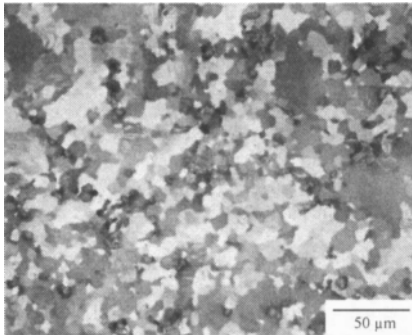


Figure 1: Microstructure of the extruded material before semi-solid processing (optical microscopy), transversal section.

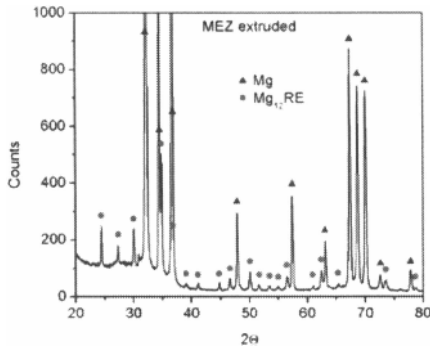


Figure 2: X-ray pattern of the MEZ alloy in its extruded condition.

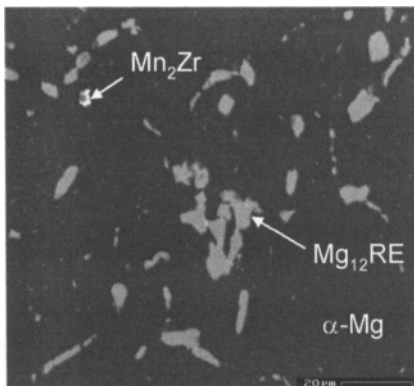


Figure 3: Microstructure of the extruded material before semi-solid processing (scanning electron microscopy), transversal section.

#### Microstructure of the Thixocast Material

The chemical composition of the MEZ alloy after thixocasting was determined by means of Inductively Coupled Plasma (ICP). The results of the analysis are shown in Table II.

Table II: Chemical composition of the processed MEZ material (in wt %) measured by ICP, magnesium based.

Fe	Mn	Ni	Zn	Zr	Ce	La	Nd	Pr	Others
0.001	0.2	0.002	0.5	0.1	1.7	0.7	0.5	0.2	0.3

Figure 4 shows the complete microstructure of the cross section of a representative thixocast plate with 10 mm thickness. In general, globular- and rosette-like mixed morphology is observed through the whole thickness of the plate. The mould has been completely filled and only small amount of pores is present. The largest grains, of the order of 150-300  $\mu m$ , are found in the core of the casting steps. The rims show smaller and more globular grains, of the order of 100  $\mu m$  and less, as well as a higher amount of finer materials. The typical microstructural features of semi-solid materials, such as spheroidized grain boundaries and secondary  $\alpha$ -grains are seen in detail in Figure 5.

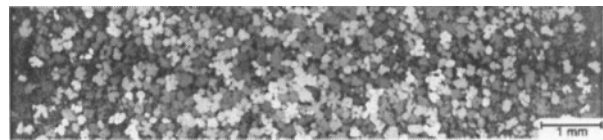


Figure 4: Complete cross section of a thixocast sample, 10 mm step (rims are at both extremes, to the left and to the right).

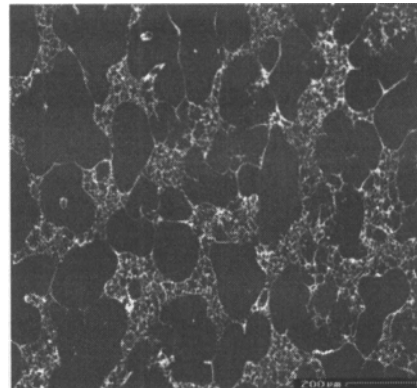


Figure 5: Microstructure of the thixocast material (scanning electron microscopy), middle of a step.

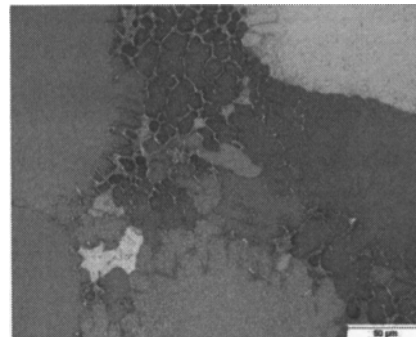


Figure 6: Closer look of the microstructure of the thixocast material (optical microscopy), middle of a step.

Figure 6 shows a closer look of the spheroidized grain boundaries and areas of small grain formation. A mixture of secondary  $\alpha$ -

grains and eutectic is formed at the grain boundaries. The small grains are typically of globular shape with about 10-15  $\mu\text{m}$  in size and often also exhibit spheroidized grain boundaries.

Creep Behavior of Thixocast Samples

The relationship between the secondary creep rate and the stress is shown for all temperatures in Figure 7. The experimental results show a reasonable fit to a straight line with the stress exponent very close to 4. The value of the stress exponent  $n$  calculated after fitting the points varies between 3.9 and 4.3.

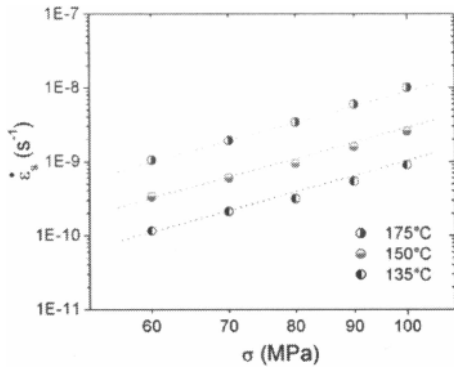


Figure 7: Creep rates versus stresses at different temperatures for the thixocast MEZ alloy (double logarithmic scale). Dotted lines indicate the fit for the determination of the stress exponent.

The temperature dependence of the secondary creep rates is shown in Figure 8 at different stresses. The activation energy determined after fitting the points has a value of 80-89 kJ/mol for all stresses, which is close to the value of grain boundary diffusion (80 kJ/mol) and is also close to the value for dislocation pipe diffusion of ~92 kJ/mol [7].

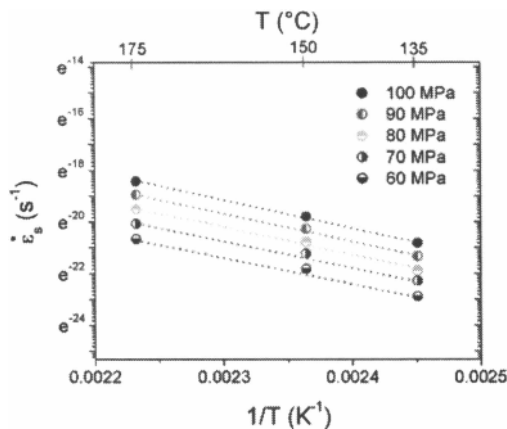


Figure 8: Creep rates versus 1/T at different stresses for the thixocast MEZ alloy (logarithmic scale). Dotted lines indicate the fit for the determination of the activation energy.

Microstructure of Thixocast Samples after Creep

At 135°C and lower stresses, the microstructure shows only sporadic primary twinning. At increasing stresses (80 MPa and

higher), Figure 9, primary twinning is significantly increased and secondary twinning is activated. As compared to 135°C, at 150°C the density of primary and secondary twinning increases in the bulk sample even at low stresses, corresponding to larger strain rates. The shape of the twinning broadens from thin lamellae to lenticular as the stress is increased. The eutectic phase appears fractured at higher stresses and low angle boundaries are already visible in some grains, Figure 10. At 175°C, low angle boundaries or substructures are developed within grains, even at low stresses. Only grains with a determined crystallographic orientation are able to develop these substructures. Overaging precipitations can also be observed. Primary and secondary twinings are also present, as well as fractured phases at high stresses.

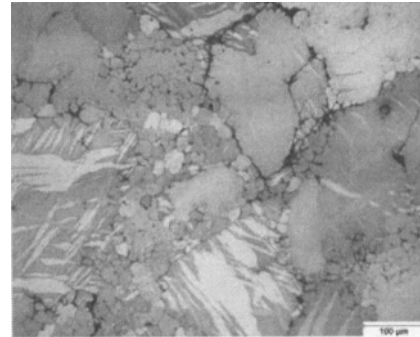


Figure 9: Representative microstructure of the thixocast MEZ alloy after creep at 135°C and 100 MPa, optical microscopy.

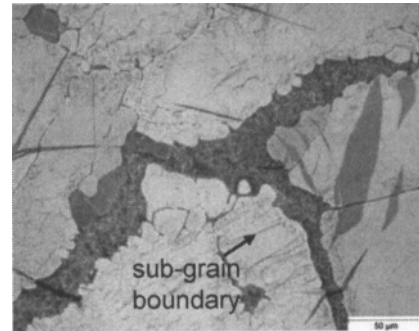


Figure 10: Representative microstructure of the thixocast MEZ alloy after creep at 150°C and 80 MPa, optical microscopy.



Figure 11: Representative microstructure of the thixocast MEZ alloy after creep at 175°C and 100 MPa, optical microscopy.

The twin formation observed already in optical microscopy is confirmed by TEM analysis of a sample crept at 175°C and 80 MPa (Figure 12a). Dislocation pinning can be discerned because of the dislocations attached to precipitations (Figure 12b). In some sections, these areas of high dislocation density show parallel lines result of dislocation slip in the basal plane (not shown here). A high number of dislocation tangles perpendicular to basal plane are observed as the result of strong dislocation climb or cross slip.

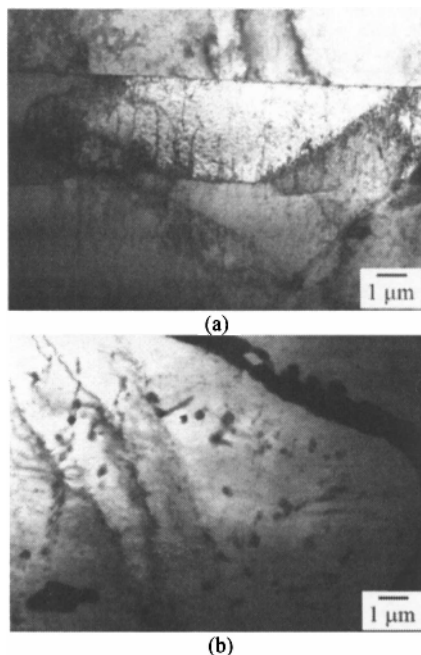


Figure 12: TEM micrographs of the thixocast MEZ alloy after creep at 175°C and 80 MPa. (a) Twin formation, (b) Dislocation pinning

### Discussion of Results

The presence of elongated grains in the extrusion direction of the as-received MEZ alloy indicates that the material did not reach a complete dynamic recrystallization after hot working, which is the reason of the bimodal grain shape. The microstructure of the thixocast material consisted of globular- or rosette-like primary  $\alpha$ -Mg grains surrounded with eutectic and secondary  $\alpha$ -Mg grains. The formation of spheroidized grain boundaries suggests that a suitable thixotropic slurry material was achieved during casting, that the heating temperature was high enough and that the casting parameters were, if not optimal, sufficient.

Slight changes during secondary creep also indicate further influences of the microstructure of thixocast alloy on the creep behavior. The slight decrease of creep rates during secondary creep at temperatures up to 175°C can be explained by an additional precipitation hardening, which was also observed by scanning and transmission microscopy.

The creep properties are mainly determined by the bimodal microstructure achieved in the thixocasting. Smaller secondary  $\alpha$ -grains delay the onset of grain movement by grain boundary sliding. In the case of thermally stable eutectic phases at the grain boundaries, like in the MEZ alloy, grain boundary sliding can

even be hindered. The grain deformation relies thus on the effect of solute elements in the matrix that cause precipitation strengthening (zinc in this case).

At temperatures up to 175°C, an activation energy of 80-89 kJ / mol and a stress exponent of 3.9 – 4.3 could be deduced. An activation energy of 81-135 kJ / mol is in general attributed to the lattice self diffusion for magnesium and its solid solutions [8]. The self diffusion corresponds to the mechanism of dislocation climb on the basal plane. For this mechanism a stress exponent of 5.5 is analytically deduced and is also measured by Tegart et al. on pure magnesium [9]. However, also slightly deviating stress exponents were measured and could be attributed to dislocation glide on the basal plane of magnesium and the corresponding dislocation climb as rate limiting step, as observed by transmission electron microscopy.

### Conclusions

Aluminum-free, zinc containing magnesium alloys can be processed in the semi-solid state as an alternative to die-casting. The thixocasting process, using extruded feedstock material reheated for short time in the semi-solid state and subsequently squeeze cast, has proven feasibility for producing relatively fine grained casts of magnesium-zinc alloys with low porosity.

The general rate determining step for creep in the MEZ alloy could be identified as dislocation climb on the basal plane for temperatures below 175°C. Due to the good quality of the cast, the material was highly resistant to tertiary creep up to temperatures of 175°C.

Although some microstructural variations were found at the different thicknesses of the thixocast plates (grain size and grain shape), a logical sequence for the minimal creep rate was obtained, fact that permitted the determination of the creep parameters. It can be concluded then that the creep behavior is driven by solution and precipitation hardening rather than by microstructural effects.

### References

1. B.R. Powell, V. Rezhets, M.P. Balogh, and A. Waldo, "The relationship between microstructure and creep behavior in AE42 magnesium die casting alloy", *Magnesium Technology 2001*, ed. J. Hryn (TMS, USA, 2001), 175-181
2. M.O. Pekguleryuz, and A.A. Kaya, "Creep resistant magnesium alloys for power train applications", *Advanced Engineering Materials*, 5 (12) (2003), 866-878
3. J.F. King, "Development of practical high temperature magnesium casting alloys", *Magnesium Alloys and their Applications*, ed. K.U. Kainer (Wiley-VCH, Germany, 2000), 15-22
4. W. Wagener, and D. Hartmann, "Feedstock material for semi-solid casting of magnesium", *6th International Conference on Semi-Solid Processing of Magnesium Alloys and Composites*, ed. G.L. Chiarmetta, and M. Rosso, (EDIMET, Italy, 2000), 301-306

5. S. Kleiner, O. Beffort, and P.J. Uggowitzer, "Microstructure evolution during reheating of an extruded Mg–Al–Zn alloy into the semisolid state", *Scripta Materialia*, 51 (5) (2004), 405-410
6. V. Kree, J. Bohlen, D. Letzig, and K.U. Kainer, "The metallographic examination of magnesium alloys", *Praktische Metallographie*, 41 (5) (2004), 233-246
7. M. Regev, E. Aghion, A. Rosen, and M. Bamberger, "Creep studies of coarse grained AZ91D magnesium castings", *Materials Science and Engineering*, A252 (1998), 6-16
8. S.S. Vagarali, and T.G. Langdon, "Deformation mechanisms in H.C.P. metals at elevated temperatures (II): Creep behaviour of a Mg - 0.8 % Al solid solution alloy", *Acta metallurgica*, 30 (1982), 1157-1170
9. W.J. McG. Tegart, "Activation energies for high temperature creep of polycrystalline magnesium", *Acta Metallurgica*, 9 (1961), 614-617